Available online at www.sciencedirect.com
ScienceDirect
Trans. Nonferrous Met. Soc. China 19(2009) 1271−1279
Transactions of Nonferrous Metals Society of China
www.tnmsc.cn

A thermodynamic approach to assess glass-forming ability of bulk metallic glasses

JI Xiu-lin (纪秀林)[1], PAN Ye(潘 冶)[2]

1. Engineering Research Center of Dredging Technology of Ministry of Education, Hohai University, Changzhou 213022, China;
2. School of Materials Science and Engineering, Southeast University, Nanjing 211189, China

Received 28 September 2008; accepted 6 March 2009

Abstract: According to the Gibbs free energy difference between liquid and crystal, a thermodynamic glass-forming ability(GFA) parameter related to characteristic temperatures, onset crystallization temperature(T_x) and liquidus temperature(T_l), was proposed for evaluating the GFA of bulk metallic glasses(BMGs). The new parameter defined as $\omega=T_l(T_l+T_x)/(T_x(T_l-T_x))$ has good correlation with the critical section thickness(Z_c) of Ca-Mg-Cu BMGs. Being verified by the glasses data, including oxide glasses, which were used to validate the former GFA parameters, ω is one of the most reliable and applicable GFA parameters among T_{rg} ($=T_g/T_l$), $\gamma(=T_x/(T_l+T_g))$, α ($=T_x/T_l$), δ ($=T_x/(T_l-T_g)$, and so on. Finally, predicting GFA of Cu-Ag-Zr-Ti and Cu-Zr-Ti-Al BMGs using ω was compared with the experimental results.

Key words: glass-forming ability; bulk metallic glass; Gibbs free energy

1 Introduction

Whether the vitrification of an alloy is easy or difficult, glass-forming ability(GFA) is vital to develop new bulk metallic glasses(BMGs). Scientific efforts for quantification of GFA have been started when the first Au-Si metallic glass was reported[1]. TURNBULL[2] identified reduced glass transition temperature(T_{rg}), which is the ratio of glass transition temperature(T_g) to liquidus temperature(T_l), as a GFA gauge. INOUE et al [3] proposed the supercooled liquid region ΔT_x ($=T_x-T_g$, where T_x is the onset crystallization temperature of the glass) to measure GFA. Since 2002, LU and LIU[4−6] have published a serial of papers to show the strongest correlation of the GFA parameter γ ($=T_x/(T_l+T_g)$) with the GFA of various glass formers among the parameters suggested so far. Therefore, γ has been frequently used to predict the GFA of alloys today.

However, the predominant situation of γ is challenged in recent two years by other GFA indicators, $\alpha(=T_x/T_l)$[7], $\delta(=T_x/(T_l-T_g)$[8], ϕ $(=T_{rg}(\Delta T_x/T_g)^{0.143})$[9], $T_{rx}(=T_x/T_s$, where T_s is onset temperature of solidification)[10], and so on. Origins of those GFA parameters mentioned above obtained from time—temperature—transformation(TTT) diagram analysis[5, 7−10] or kinetics analysis, such as viscosity[11], fragility[9] and homogenous nucleation and growth[4, 8]. Lately, LU et al[1] restated that γ was still the best GFA indicator in terms of reliability and applicability.

In this work, based on thermodynamic analysis, mainly Gibbs free energy difference between liquid and crystal, a new GFA parameter was proposed and the new glass criterion was validated with lots of experimental data to assess the GFA of BMGs.

2 Origins of new parameter

Gibbs free energy difference(ΔG_{l-s}) between liquid and crystal means the driving force of crystallization. In a supercooled alloying liquid, the less ΔG_{l-s} means the more stable and the better GFA of the liquid. Thus, ΔG_{l-s} plays an important role in appraising the GFA of BMGs and the GFA parameter maybe has a solid interrelationship with ΔG_{l-s}. In this way, a new GFA indicator was developed by this approach.

Scientific efforts for ΔG_{l-s} estimation of the supercooled alloying liquid have started for a long time and many approximate expressions of ΔG_{l-s} have been derived [12−14]. The expression developed by THOMPSON and

Corresponding author: JI Xiu-lin; Tel: +86-519-85191969; E-mail: xiulinji@gmail.com
DOI: 10.1016/S1003-6326(08)60438-0

SPAEPEN[12] is one of the most important and reliable:

$$\Delta G_{\mathrm{l-s}}=\frac{2\Delta H_{\mathrm{m}}T(T_{\mathrm{m}}-T)}{T_{\mathrm{m}}(T_{\mathrm{m}}+T)} \tag{1}$$

where T_{m} is the melting temperature; ΔH_{m} is the enthalpy of fusion; and T is the temperature of the supercooled liquid.

As discussed above, GFA of metallic glasses is associated with $\Delta G_{\mathrm{l-s}}$. So, their relationship can be expressed as follows:

$$\mathrm{GFA}\propto\frac{1}{\Delta G_{\mathrm{l-s}}}\propto\frac{T_{\mathrm{m}}(T_{\mathrm{m}}+T)}{\Delta H_{\mathrm{m}}T(T_{\mathrm{m}}-T)} \tag{2}$$

At slower cooling rates, the glass freezes at lower temperature. But the glass produced at higher cooling rates undergoes structural relaxation readily at lower temperature[15]. So, T_{g} detected from DSC (differential scanning calorimetry) is different from the actual freezing temperature of an metallic glass. But the expression of $\Delta G_{\mathrm{l-s}}$ is derived from continuous cooling process. Therefore, it is not surprising that the GFA parameter directly using Eq.(2) has no good correlation with GFA.

For glass transition of an alloying system, two equilibrium states, amorphous and liquid states, should be emphasized. From the viewpoint of heating process, the glass is still in amorphous state before system temperature exceeds T_{x} and the alloying system is not in a real liquid state before it reaches T_{l}. That is to say, T_{x} and T_{l} are thermal stability gauges of the glass and the liquid, respectively[7]. Thus, T_{l} but T_{m} characterizes the temperature of a liquid state and T_{x} but T_{g} characterizes the temperature of an amorphous state. Therefore, T and T_{m} in Eq.(2) are substituted by T_{x} and T_{l}, respectively, meaning that GFA is in inverse proportion to the Gibbs free energy difference of the alloying system from T_{l} to T_{x}. So, the following expression can be obtained from Eq.(2):

$$\mathrm{GFA}\propto\frac{1}{\Delta H_{\mathrm{m}}}\cdot\frac{T_{\mathrm{l}}(T_{\mathrm{l}}+T_{\mathrm{x}})}{T_{\mathrm{x}}(T_{\mathrm{l}}-T_{\mathrm{x}})} \tag{3}$$

If there is no inner relationship between ΔH_{m} and T_{l} (or T_{x}), the above expression can be simplified as

$$\mathrm{GFA}\propto\frac{T_{\mathrm{l}}(T_{\mathrm{l}}+T_{\mathrm{x}})}{T_{\mathrm{x}}(T_{\mathrm{l}}-T_{\mathrm{x}})} \tag{4}$$

Hence, the new parameter ω for inferring the relative GFA among BMGs is defined as

$$\omega=\frac{T_{\mathrm{l}}(T_{\mathrm{l}}+T_{\mathrm{x}})}{T_{\mathrm{x}}(T_{\mathrm{l}}-T_{\mathrm{x}})} \tag{5}$$

To reveal the validity of ω as a GFA parameter, Eq.(5) is deduced as:

$$\omega=\frac{T_{\mathrm{l}}(T_{\mathrm{l}}+T_{\mathrm{x}})}{T_{\mathrm{x}}(T_{\mathrm{l}}-T_{\mathrm{x}})}=\frac{T_{\mathrm{l}}}{T_{\mathrm{l}}-T_{\mathrm{x}}}\cdot\frac{T_{\mathrm{l}}+T_{\mathrm{x}}}{T_{\mathrm{x}}}=\frac{T_{\mathrm{l}}/T_{\mathrm{x}}}{T_{\mathrm{l}}/T_{\mathrm{x}}-1}\cdot\left(\frac{T_{\mathrm{l}}}{T_{\mathrm{x}}}+1\right) \tag{6}$$

Compared with T_{l}, the difference between T_{x} and T_{g} is very little, usually less than 5% T_{l} for the characteristic temperatures of BMGs. Therefore, the GFA parameters, $T_{\mathrm{rg}}=T_{\mathrm{g}}/T_{\mathrm{l}}$[2], $\gamma=T_{\mathrm{x}}/(T_{\mathrm{g}}+T_{\mathrm{l}})$[4−6] and $\alpha=T_{\mathrm{x}}/T_{\mathrm{l}}$[7] are close, respectively, to $T_{\mathrm{x}}/T_{\mathrm{l}}$, $T_{\mathrm{x}}/(T_{\mathrm{x}}+T_{\mathrm{l}})$ and $T_{\mathrm{x}}/T_{\mathrm{l}}$. All the GFA parameters, T_{rg}, γ and α can be treated as functions of $T_{\mathrm{x}}/T_{\mathrm{l}}$. On the other hand, Eq.(6) indicates that ω is also the function of $T_{\mathrm{x}}/T_{\mathrm{l}}$. And the positive correlation between ω and α is illustrated in Fig.1. So, ω not only has the accordant trends of GFA description with α, but also expands the difference of values between descriptive parameters. And it may be more effective than other GFA parameters.

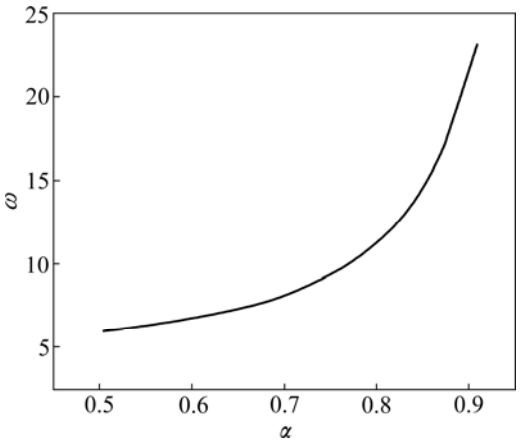

Fig.1 Function relationship between GFA parameters ω and α

3 Results and discussion

3.1 Correlation between new parameters and GFA

The most direct GFA indicator is the critical cooling rate(R_{c}) and the critical section thickness(Z_{c}). Unfortunately, it is very difficult to measure R_{c} experimentally and Z_{c} is rough. Table 1 shows the glass transition temperature(T_{g}), onset crystallization temperature(T_{x}), liquidus temperature(T_{l}) and Z_{c} of Ca-Mg-Cu BMGs. The data in Table 1 were obtained from Ref.[16]. And the calculated GFA indicators (γ and ω) are also listed in Table 1. The relationships between ω, γ and Z_{c} are shown in Fig.2. In order to reveal how closely the GFA indicators (γ and ω) correspond to the actual experimental data of Z_{c}, the statistical correlation parameter, R^2, was also computed. The higher the R^2, the more reliable the GFA parameter. As shown in Fig.2, R^2

Table 1 T_g, T_x, T_l, T_m, Z_c, ΔH_m and calculated γ and ω for Ca-Mg-Cu BMGs

Alloy	T_g/K	T_x/K	T_l/K	T_m/K	Z_c/mm	ΔH_x/(J·g^{-1})	γ	ω
$Ca_{40}Mg_{30}Cu_{30}$	395	430	694	647	0.5	91	0.395	6.872
$Ca_{40}Mg_{25}Cu_{35}$	399	436	680	650	4.0	89	0.404	7.133
$Ca_{45}Mg_{30}Cu_{25}$	401	436	717	627	1.0	94	0.390	6.748
$Ca_{45}Mg_{25}Cu_{30}$	400	438	678	627	6.0	132	0.406	7.198
$Ca_{45}Mg_{19}Cu_{36}$	399	428	714	649	0.5	106	0.385	6.661
$Ca_{47.5}Mg_{22.5}Cu_{30}$	399	440	673	625	6.0	154	0.410	7.306
$Ca_{50}Mg_{30}Cu_{20}$	402	439	731	627	2.0	104	0.387	6.672
$Ca_{50}Mg_{25}Cu_{25}$	400	439	655	627	9.0	129	0.416	7.557
$Ca_{50}Mg_{22.5}Cu_{27.5}$	400	442	663	627	10.0	150	0.416	7.500
$Ca_{50}Mg_{20}Cu_{30}$	401	442	690	628	8.0	139	0.405	7.126
$Ca_{53}Mg_{23}Cu_{24}$	406	439	655	627	7.0	134	0.414	7.557
$Ca_{55}Mg_{25}Cu_{30}$	398	428	668	627	8.0	125	0.402	7.127
$Ca_{55}Mg_{20}Cu_{25}$	399	426	720	628	2.0	106	0.381	6.588
$Ca_{55}Mg_{15}Cu_{30}$	397	437	706	626	3.0	137	0.396	6.865
$Ca_{55}Mg_{10}Cu_{35}$	397	422	770	629	0.5	98	0.362	6.250
$Ca_{58}Mg_{18}Cu_{24}$	388	426	667	628	6.0	119	0.404	7.101
$Ca_{60}Mg_{25}Cu_{15}$	390	416	676	628	2.0	102	0.390	6.825
$Ca_{60}Mg_{20}Cu_{20}$	387	412	678	629	4.0	105	0.387	6.743
$Ca_{60}Mg_{15}Cu_{25}$	396	428	687	627	1.0	99	0.395	6.910
$Ca_{60}Mg_{13}Cu_{27}$	394	426	701	628	1.0	98	0.389	6.744
$Ca_{65}Mg_{25}Cu_{10}$	405	429	691	637	0.5	96	0.391	6.886
$Ca_{65}Mg_{20}Cu_{15}$	386	405	679	636	2.0	101	0.380	6.633
$Ca_{65}Mg_{15}Cu_{20}$	383	409	682	630	4.0	115	0.384	6.664
$Ca_{65}Mg_{10}Cu_{25}$	388	420	711	630	2.0	114	0.382	6.579
$Ca_{65}Mg_5Cu_{30}$	403	424	757	630	0.5	89	0.366	6.332
$Ca_{70}Mg_{20}Cu_{10}$	356	385	702	659	0.5	87	0.364	6.252
$Ca_{70}Mg_{10}Cu_{20}$	385	407	713	670	1.0	107	0.371	6.412

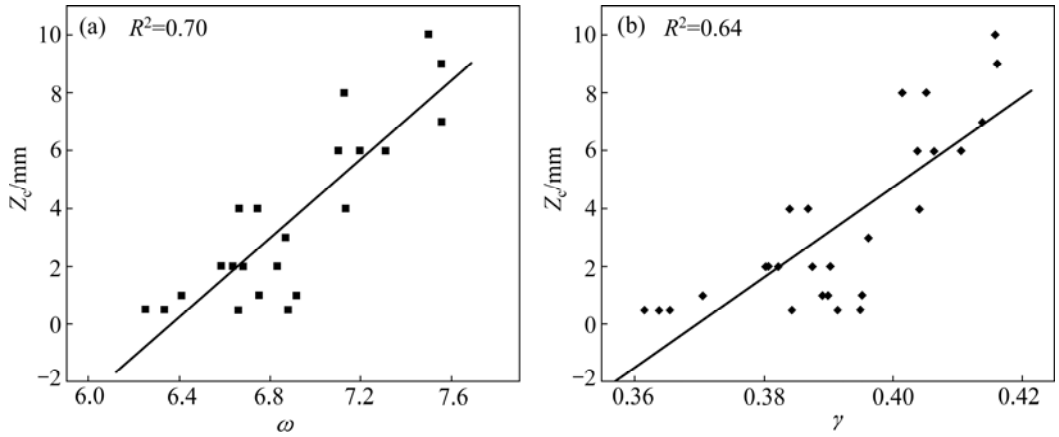

Fig.2 Correlation between Z_c and ω (a), γ (b) for Ca-Mg-Cu BMGs

of ω is 0.70, but the corresponding R^2 of γ is 0.64, indicating the new GFA parameter ω is more reliable than γ for Ca-Mg-Cu BMGs.

3.2 Comparison of ω and other GFA parameters

To verify the reliability of the new GFA parameter and to compare it with others, more BMGs data with

their characteristic temperatures (T_g, T_x and T_l) and Z_c, together with more calculated GFA parameters are listed in Table 2. The data in Table 2 were obtained from Table 1 in Ref.[4] and Table 1 in Ref.[8], which are used to interpret γ and α. The relationships between GFA indicators (T_{rg}, γ, α, δ, ϕ and ω) and the actual experimental data of Z_c, are shown in Fig.3. By comparing R^2 of every GFA indicator shown in Figs.3(a)−(f), R^2 of ω is obviously higher than others, and the order of GFA indicators from the best to the worst is ω, δ, α, ϕ, γ and T_{rg}. This result suggests the ω is the best GFA parameter. The relationship between the GFA and ω for these BMGs can be expressed as

$$Z_c=-77.98+11.93\omega \quad (7)$$

Besides T_{rg}, γ, α, δ and ϕ, other GFA parameters, such as ΔT_{rg} ($=(T_x-T_g)/(T_l-T_g)$)[17], ΔT_x, T_{rgx} ($=(T_gT_x)/(T_lT_m)$)[18] and K_{gl} ($=(T_x-T_g)/(T_m-T_x)$)[19] are also compared with ω. R^2 of ΔT_{rg} and ΔT_x calculated with data in Table 2 are 0.27 and 0.13, respectively, which are clearly lower than 0.53 of ω. From the viewpoint of emphasis on the two states, the relationships between GFA and those GFA parameters which import other characteristic temperatures beyond the amorphous and the liquid state will be injured. For example, T_g/T_l is a better representation of GFA than T_g/T_m[20]. R^2 of T_{rgx} and K_{gl} calculated with data in Table 1 are 0.53 and 0.42, respectively, which are obviously lower than 0.64 of γ and 0.70 of ω. On the other hand, except α and ω, all other GFA parameters mentioned above need the knowledge of T_g or T_s. However, T_g is not usually available for some glasses[7] and T_s needs to be measured during cooling of liquid, which increases the operational complexity. Based on above comparison, it can be concluded that ω is one of the most reliable and applicable GFA parameters.

3.3 Comparison of ω in glasses including oxides

To verify the applicability of the new GFA parameter, T_g, T_x, T_l and R_c of some BMGs and oxide glasses are listed in Table 3, together with the calculated GFA parameters. The data of BMGs and oxide glasses in Table 3 were obtained from Table 3 in Ref.[4] and Table 2 in Ref.[6], respectively, which are applied to interpreting γ. According to the data in Table 3, six plots of the critical cooling rate as the functions of the parameters, T_{rg}, γ, α, δ, ϕ and ω, respectively, are shown in Fig.4. The statistical factor R^2 for these regressions are

Table 2 T_g, T_x, T_l, Z_c and calculated T_{rg}, γ, α, δ, ϕ and ω for reported BMGs

Alloy	T_g/K	T_x/K	T_l/K	Z_c/mm	T_{rg}	γ	α	δ	ϕ	ω
$Mg_{80}Ni_{10}Nd_{10}$	454.2	470.5	878.0	0.6	0.517	0.353	0.536	1.110	0.321	6.175
$Mg_{75}Ni_{15}Nd_{10}$	450.0	470.4	789.8	2.8	0.570	0.379	0.596	1.384	0.366	6.625
$Mg_{70}Ni_{15}Nd_{15}$	467.1	489.4	844.3	1.5	0.553	0.373	0.580	1.297	0.358	6.483
$Mg_{65}Ni_{20}Nd_{15}$	459.3	501.4	804.9	3.5	0.571	0.397	0.623	1.451	0.405	6.909
$Mg_{65}Cu_{25}Y_{10}$	424.5	479.4	770.9	7.0	0.551	0.401	0.622	1.384	0.411	6.897
$Zr_{65}Al_{7.5}Cu_{17.5}Ni_{10}$	656.5	735.6	1 167.6	16.0	0.562	0.403	0.630	1.439	0.415	6.993
$Zr_{57}Ti_5Al_{10}Cu_{20}Ni_8$	676.7	720.0	1 145.2	10.0	0.591	0.395	0.629	1.537	0.399	6.977
$Zr_{41.2}Ti_{13.8}Cu_{12.5}Ni_{10}Be_{22.5}$	623.0	672.0	996.0	50.0	0.626	0.415	0.675	1.802	0.435	7.630
$La_{55}Al_{25}Ni_{20}$	490.8	555.1	941.3	3.0	0.521	0.388	0.590	1.232	0.390	6.570
$La_{55}Al_{25}Ni_{10}Cu_{10}$	467.4	547.2	835.0	5.0	0.560	0.420	0.655	1.489	0.435	7.329
$La_{55}Al_{25}Cu_{20}$	455.9	494.8	896.1	3.0	0.509	0.366	0.552	1.124	0.358	6.277
$La_{55}Al_{25}Ni_5Cu_{10}Co_5$	465.2	541.8	822.5	9.0	0.566	0.421	0.659	1.516	0.437	7.378
$La_{66}Al_{14}Cu_{20}$	395.0	449.0	731.0	2.0	0.540	0.399	0.614	1.336	0.407	6.812
$Pd_{40}Cu_{30}Ni_{10}P_{20}$	576.9	655.8	836.0	72.0	0.690	0.464	0.784	2.531	0.519	10.553
$Pd_{81.5}Cu_2Si_{16.5}$	633.0	670.0	1 097.3	2.0	0.577	0.387	0.611	1.443	0.384	6.774
$Pd_{79.5}Cu_4Si_{16.5}$	635.0	675.0	1 086.0	0.8	0.585	0.392	0.622	1.497	0.394	6.894
$Pd_{77.5}Cu_6Si_{16.5}$	637.0	678.0	1 058.1	1.5	0.602	0.400	0.641	1.610	0.407	7.128
$Pd_{77}Cu_6Si_{17}$	642.4	686.4	1 128.4	2.0	0.569	0.388	0.608	1.412	0.388	6.750
$Pd_{73.5}Cu_{10}Si_{16.5}$	645.0	685.0	1 135.9	2.0	0.568	0.385	0.603	1.395	0.382	6.697
$Pd_{71.5}Cu_{12}Si_{16.5}$	652.0	680.0	1 153.6	2.0	0.565	0.377	0.589	1.356	0.360	6.568
$Pd_{40}Ni_{40}P_{20}$	590.0	671.0	991.0	25.0	0.595	0.424	0.677	1.673	0.448	7.671
$Nd_{60}Al_{15}Ni_{10}Cu_{10}Fe_5$	430.0	475.0	779.0	5.0	0.552	0.393	0.610	1.361	0.400	6.765
$Nd_{61}Al_{11}Ni_8Co_5Cu_{15}$	445.0	469.0	744.0	6.0	0.598	0.394	0.630	1.569	0.394	6.997

Continue

Alloy	T_g/K	T_x/K	T_l/K	Z_c/mm	T_{rg}	γ	α	δ	ϕ	ω
$Cu_{60}Zr_{30}Ti_{10}$	713.0	763.0	1 151.0	4.0	0.619	0.409	0.663	1.742	0.424	7.442
$Cu_{54}Zr_{27}Ti_9Be_{10}$	720.0	762.0	1 130.0	5.0	0.637	0.412	0.674	1.859	0.424	7.624
$Ti_{34}Zr_{11}Cu_{47}Ni_8$	698.4	727.2	1 169.2	4.5	0.597	0.389	0.622	1.545	0.379	6.898
$Ti_{50}Ni_{24}Cu_{20}B_1Si_2Sn_3$	726.0	800.0	1 310.0	1.0	0.554	0.393	0.611	1.370	0.400	6.775
$Cu_{55}Zr_{42.5}Ga_{2.5}$	709.0	762.0	1 199.0	1.0	0.591	0.399	0.636	1.555	0.408	7.061
$Cu_{57.5}Zr_{37.5}Ga_5$	745.0	785.0	1 241.0	1.0	0.600	0.395	0.633	1.583	0.395	7.024
$Cu_{57.5}Zr_{40}Ga_{2.5}$	723.0	776.0	1 198.0	1.5	0.604	0.404	0.648	1.634	0.415	7.222
$Cu_{42.5}Zr_{40}Ga_{7.5}$	744.0	777.0	1 218.0	1.5	0.611	0.396	0.638	1.639	0.391	7.091
$Cu_{55}Zr_{40}Ga_5$	736.0	779.0	1 193.0	2.0	0.617	0.404	0.653	1.705	0.411	7.295
$Cu_{52.5}Zr_{42.5}Ga_5$	733.0	777.0	1 187.0	2.0	0.618	0.405	0.655	1.711	0.413	7.318
$Cu_{46}Zr_{54}$	696.0	746.0	1 201.0	2.0	0.580	0.393	0.621	1.477	0.398	6.889
$Cu_{46}Zr_{47}Al_7$	705.0	781.0	1 163.0	3.0	0.606	0.418	0.672	1.705	0.441	7.578
$Cu_{46}Zr_{37}Al_7Y_{10}$	665.0	743.0	1 118.0	4.0	0.595	0.417	0.665	1.640	0.438	7.467
$Cu_{46}Zr_{45}Al_7Y_{12}$	693.0	770.0	1 143.0	8.0	0.606	0.419	0.674	1.711	0.443	7.613
$Cu_{46}Zr_{42}Al_7Y_5$	672.0	772.0	1 113.0	10.0	0.604	0.432	0.694	1.751	0.460	7.970
$Y_{56}Al_{24}Co_{20}$	636.0	690.0	1 085.0	2.0	0.586	0.401	0.636	1.537	0.412	7.066
$Y_{36}Sc_{20}Al_{24}Co_{20}$	645.0	760.0	1 034.0	25.0	0.624	0.453	0.735	1.954	0.487	8.908
$Y_{36}Sc_{20}Al_{24}Co_{10}Ni_{10}$	645.0	731.0	1010.0	25.0	0.639	0.442	0.724	2.003	0.479	8.622
$Ca_{70}Mg_{15}Zn_{15}$	371.0	389.0	686.0	5.0	0.541	0.368	0.567	1.235	0.351	6.383
$Ca_{65}Mg_{10}Zn_{25}$	378.0	414.0	686.0	6.0	0.551	0.389	0.603	1.344	0.394	6.701
$Ca_{65}Mg_{20}Zn_{15}$	380.0	405.0	666.0	9.0	0.571	0.387	0.608	1.416	0.387	6.748
$Ca_{60}Mg_{15}Zn_{25}$	382.0	426.0	676.0	11.0	0.565	0.403	0.630	1.449	0.415	6.995
$Ca_{65}Mg_{15}Zn_{20}$	379.0	412.0	624.0	15.0	0.607	0.411	0.660	1.682	0.428	7.401
$Mg_{65}Cu_{25}Er_{10}$	422.0	480.0	766.0	3.0	0.551	0.404	0.627	1.395	0.415	6.952
$Mg_{65}Cu_{15}Ag_{10}Er_{10}$	427.0	465.0	733.0	6.0	0.583	0.401	0.634	1.520	0.412	7.046
$Mg_{65}Cu_{7.5}Ni_{7.5}Zn_5Ag_5Y_{10}$	426.0	464.0	717.0	9.0	0.594	0.406	0.647	1.595	0.421	7.213
$Ti_{50}Ni_{15}Cu_{32}Sn_3$	686.0	759.0	1 283.0	1.0	0.535	0.385	0.592	1.271	0.388	6.587
$Ti_{50}Ni_{15}Cu_{25}Sn_3Be_7$	688.0	733.0	1 207.0	2.0	0.570	0.387	0.607	1.412	0.386	6.739
$Ti_{45}Ni_{15}Cu_{25}Sn_3Be_7Zr_5$	680.0	741.0	1 142.0	5.0	0.595	0.407	0.649	1.604	0.422	7.237
$Ti_{40}Zr_{25}Ni_8Cu_9Be_{18}$	624.0	668.0	1 009.0	8.0	0.618	0.409	0.662	1.735	0.423	7.428
$Ti_{50}Cu_{42.5}Ni_{7.5}$	670.0	708.0	1 226.0	0.2	0.546	0.373	0.577	1.273	0.363	6.465
$Ti_{47.5}Zr_{2.5}Cu_{42.5}Ni_{7.5}$	673.0	720.0	1 225.0	1.5	0.549	0.379	0.588	1.304	0.375	6.553
$Ti_{42.5}Zr_{2.5}Hf_5Cu_{42.5}Ni_{7.5}$	677.0	726.0	1 203.0	2.5	0.563	0.386	0.603	1.380	0.387	6.701
$Ti_{41.5}Zr_{2.5}Hf_5Cu_{42.5}Ni_{7.5}Si_1$	680.0	730.0	1 199.0	5.0	0.567	0.389	0.609	1.407	0.390	6.755
$Au_{55}Cu_{25}Si_{20}$	348.0	383.0	654.0	0.5	0.532	0.382	0.586	1.252	0.383	6.534
$Au_{46}Ag_5Cu_{29}Si_{20}$	395.0	420.0	664.0	1.0	0.595	0.397	0.633	1.561	0.401	7.024
$Au_{52}Pd_{2.3}Cu_{29.2}Si_{16.5}$	393.0	427.0	651.0	2.0	0.604	0.409	0.656	1.655	0.425	7.337
$Au_{49}Ag_{5.5}Pd_{2.3}Cu_{26.9}Si_{16.3}$	401.0	459.0	644.0	5.0	0.623	0.439	0.713	1.889	0.472	8.365
$Ce_{60}Al_{10}Ni_{10}Cu_{20}$	374.0	441.0	672.0	1.0	0.557	0.422	0.656	1.480	0.435	7.342
$Ce_{57}Al_{10}Ni_{12.5}Cu_{15.5}Nb_5$	369.0	415.0	677.0	2.0	0.545	0.397	0.613	1.347	0.405	6.799
$Ce_{70}Al_{10}Ni_{10}Cu_{10}$	359.0	377.0	714.0	3.0	0.503	0.351	0.528	1.062	0.328	6.131
$Ce_{65}Al_{12.5}Ni_{12.5}Cu_{10}$	371.0	402.0	709.0	3.0	0.523	0.372	0.567	1.189	0.367	6.383
$Ce_{60}Al_{15}Ni_{15}Cu_{10}$	390.0	468.0	685.0	3.0	0.569	0.435	0.683	1.586	0.452	7.777
$Ce_{65}Al_{10}Ni_{10}Cu_{10}Nb_5$	359.0	384.0	702.0	5.0	0.511	0.362	0.547	1.120	0.349	6.243

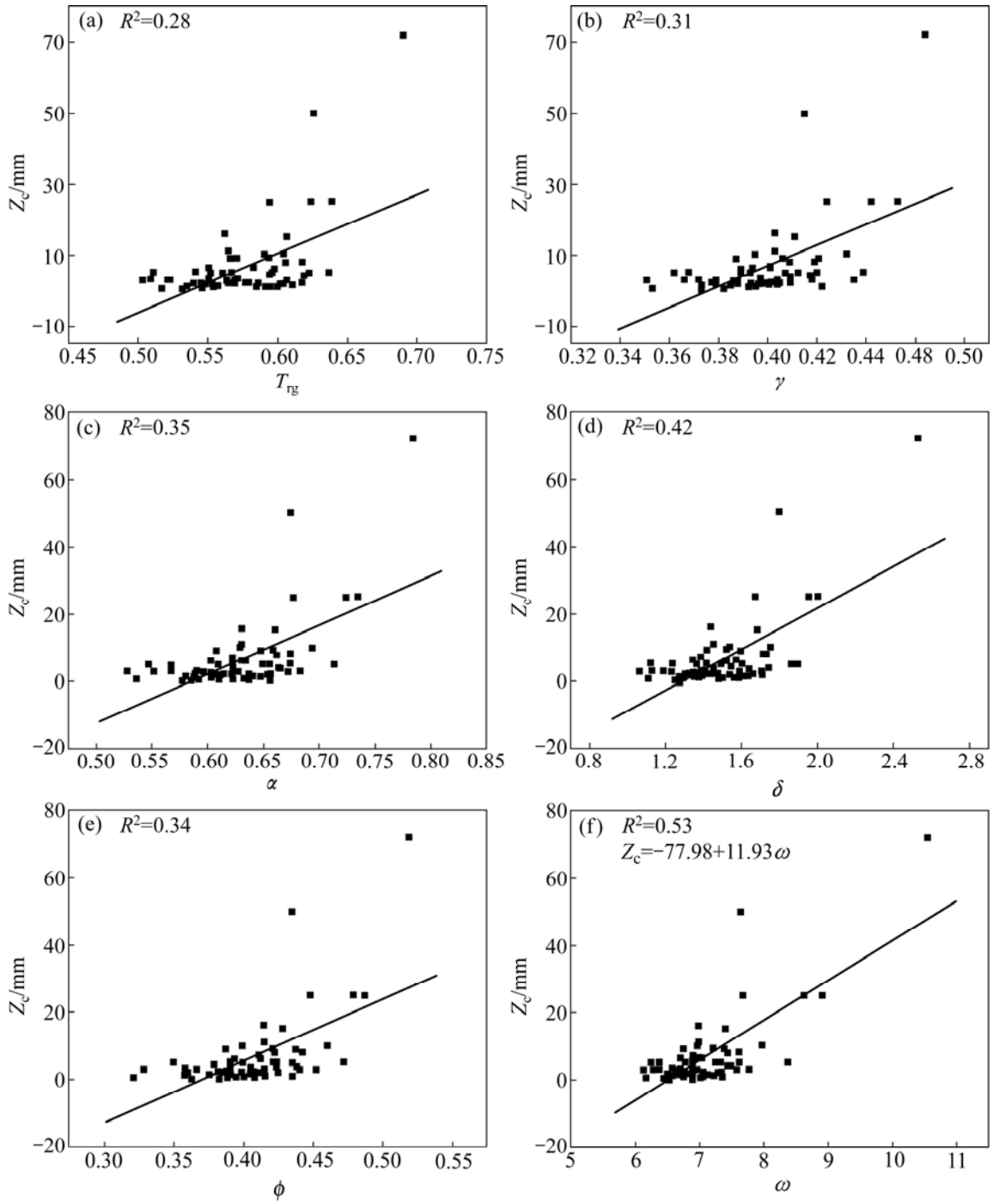

Fig.3 Correlations between Z_c and T_{rg} (a), γ (b), α (c), δ (d), ϕ (e) and ω (f) for BMGs

high among which R^2 of ω is the highest. This suggests a reliable relationship between the GFA and ω for these BMGs and oxide glasses. And this relationship is expressed in an approximation formula:

$$\lg R_c=6.72-0.80\omega \quad (8)$$

3.4 Applications of ω in bulk metallic glasses

As an applicable GFA parameter, ω should indicate the actual GFA of BMGs. A centimeter-diameter Cu-based BMG had been developed[21]. Their experimental data and the calculated values are listed in Table 4. Values of ω and the calculated values of Z_c are computed with Eq.(5) and Eq.(7), respectively. The relationship between the experimental values of Z_c (Z_c^{Exp}) and the calculated values of Z_c (Z_c^{Cal}) is shown in Fig.5. Although the values of Z_c^{Exp} are not usually equal to the values of Z_c^{Cal} for every alloying composition, they present a solid linear relationship with 0.92 of R^2. Therefore, with the knowledge of T_x and T_l, the critical section thickness and the critical cooling rate of the alloy

Table 3 T_g, T_x, T_l, R_c and calculated T_{rg}, γ, α, δ, ϕ and ω for reported BMGs and oxide glasses

Sample	T_g/K	T_x/K	T_l/K	R_c/mm	T_{rg}	γ	α	δ	φ	ω
$Mg_{80}Ni_{10}Nd_{10}$	454.2	470.5	878.0	1251.4	0.517	0.353	0.536	1.110	0.321	6.175
$Mg_{75}Ni_{15}Nd_{10}$	450.0	470.4	789.8	46.1	0.570	0.379	0.596	1.384	0.366	6.625
$Mg_{70}Ni_{15}Nd_{15}$	467.1	489.4	844.3	178.2	0.553	0.373	0.580	1.297	0.358	6.483
$Mg_{65}Ni_{20}Nd_{15}$	459.3	501.4	804.9	30.0	0.571	0.397	0.623	1.451	0.405	6.909
$Mg_{65}Cu_{25}Y_{10}$	424.5	479.4	770.9	50.0	0.551	0.401	0.622	1.384	0.411	6.897
$Zr_{65}Al_{7.5}Cu_{17.5}Ni_{10}$	656.5	735.6	1 167.6	1.5	0.562	0.403	0.630	1.439	0.415	6.993
$Zr_{57}Ti_5Al_{10}Cu_{20}Ni_8$	676.7	720.0	1 145.2	10.0	0.591	0.395	0.629	1.537	0.399	6.977
$Zr_{41.2}Ti_{13.8}Cu_{12.5}Ni_{10}Be_{22.5}$	623.0	672.0	996.0	1.4	0.626	0.415	0.675	1.802	0.435	7.630
$La_{55}Al_{25}Ni_{20}$	490.8	555.1	941.3	67.5	0.521	0.388	0.590	1.232	0.390	6.570
$La_{55}Al_{25}Ni_{10}Cu_{10}$	467.4	547.2	835.0	22.5	0.560	0.420	0.655	1.489	0.435	7.329
$La_{55}Al_{25}Cu_{20}$	455.9	494.8	896.1	72.3	0.509	0.366	0.552	1.124	0.358	6.277
$La_{55}Al_{25}Ni_5Cu_{10}Co_5$	465.2	541.8	822.5	18.8	0.566	0.421	0.659	1.516	0.437	7.378
$La_{66}Al_{14}Cu_{20}$	395.0	449.0	731.0	37.5	0.540	0.399	0.614	1.336	0.407	6.812
$Pd_{40}Cu_{30}Ni_{10}P_{20}$	576.9	655.8	836.0	0.1	0.690	0.464	0.784	2.531	0.519	10.553
$Pd_{81.5}Cu_2Si_{16.5}$	633.0	670.0	1 097.3	500.0	0.577	0.387	0.611	1.443	0.384	6.774
$Pd_{79.5}Cu_4Si_{16.5}$	635.0	675.0	1 086.0	100.0	0.585	0.392	0.622	1.497	0.394	6.894
$Pd_{77.5}Cu_6Si_{16.5}$	637.0	678.0	1 058.1	125.0	0.602	0.400	0.641	1.610	0.407	7.128
$Pd_{71.5}Cu_{12}Si_{16.5}$	652.0	680.0	1 153.6	0.2	0.565	0.377	0.589	1.356	0.360	6.568
$Ti_{34}Zr_{11}Cu_{47}Ni_8$	698.4	727.2	1 169.2	100.0	0.597	0.389	0.622	1.545	0.379	6.898
$45Na_2O$-$45B_2O_3$-$10Al_2O_3$	627	732	1 182	100	0.530	0.405	0.619	1.319	0.411	6.868
$44Na_2O$-$44B_2O_3$-$12Al_2O_3$	632	739	1 173	24.4	0.539	0.409	0.630	1.366	0.418	6.993
$43Na_2O$-$43B_2O_3$-$14Al_2O_3$	637	735	1 157.5	16.1	0.550	0.410	0.635	1.412	0.421	7.054
$42Na_2O$-$42B_2O_3$-$16Al_2O_3$	653	748	1 130	6.5	0.578	0.420	0.662	1.568	0.439	7.427
$41Na_2O$-$41B_2O_3$-$18Al_2O_3$	655	763	1 117	1.1	0.586	0.431	0.683	1.652	0.453	7.775
$40Na_2O$-$40B_2O_3$-$20Al_2O_3$	656	765	1 148	1.1	0.571	0.424	0.666	1.555	0.442	7.495
$37Na_2O$-$37B_2O_3$-$26Al_2O_3$	672	773	1 205	2	0.558	0.412	0.641	1.450	0.425	7.138
$36Na_2O$-$36B_2O_3$-$28Al_2O_3$	682	759	1 235	5.3	0.552	0.396	0.615	1.373	0.404	6.816
$35Na_2O$-$35B_2O_3$-$30Al_2O_3$	696	776	1 251	9.4	0.556	0.399	0.620	1.398	0.408	6.879
$34Na_2O$-$34B_2O_3$-$32Al_2O_3$	709	823	1 252	9.6	0.566	0.420	0.657	1.516	0.436	7.358
$33.4Na_2O$-$33.4B_2O_3$ -$33.2Al_2O_3$	736	887	1 262	3.3	0.583	0.444	0.703	1.686	0.465	8.153
$15CaO$-$22Al_2O_3$-$63SiO_2$*	1173	1 298	1 493	3.4×10^{-6}	0.786	0.487	0.869	4.056	0.570	16.463
$15CaO$-$22Al_2O_3$-$63SiO_2$-$2Na_2O$*	1133	1 253	1 476	1.6×10^{-5}	0.768	0.480	0.849	3.653	0.557	14.416
$15CaO$-$22Al_2O_3$-$63SiO_2$-$4TiO_2$*	1158	1 258	1 482	1.6×10^{-5}	0.781	0.477	0.849	3.883	0.550	14.410
$15CaO$-$22Al_2O_3$-$63SiO_2$-$2Na_2O$-$4TiO_2$*	1133	1 201	1 486	3.2×10^{-4}	0.762	0.459	0.808	3.402	0.510	11.665
Na_2O-$2SiO_2$	687	915	1 173	1.7×10^{-3}	0.586	0.492	0.780	1.883	0.500	10.375
SiO_2-43CaO	1017	1 178	1 773	2.3×10^{-2}	0.574	0.422	0.664	1.558	0.441	7.465
SiO_2-50CaO	1017	1 154	1 817	2.6×10^{-1}	0.560	0.407	0.635	1.443	0.420	7.056
SiO_2-54.8CaO	1076	1 173	1 753	5.1	0.614	0.415	0.669	1.733	0.435	7.539
Li_2O-$2SiO_2$	738	899	1 339	0.2	0.551	0.433	0.671	1.496	0.443	7.576
BaO-$2SiO_2$	974	1 137	1 690	3	0.576	0.427	0.673	1.588	0.446	7.598
Na_2O-2CaO-$3SiO_2$	849	991	1 537	4.3	0.552	0.415	0.645	1.440	0.428	7.181

* means the data in mass fraction; the other data are in molar fraction.

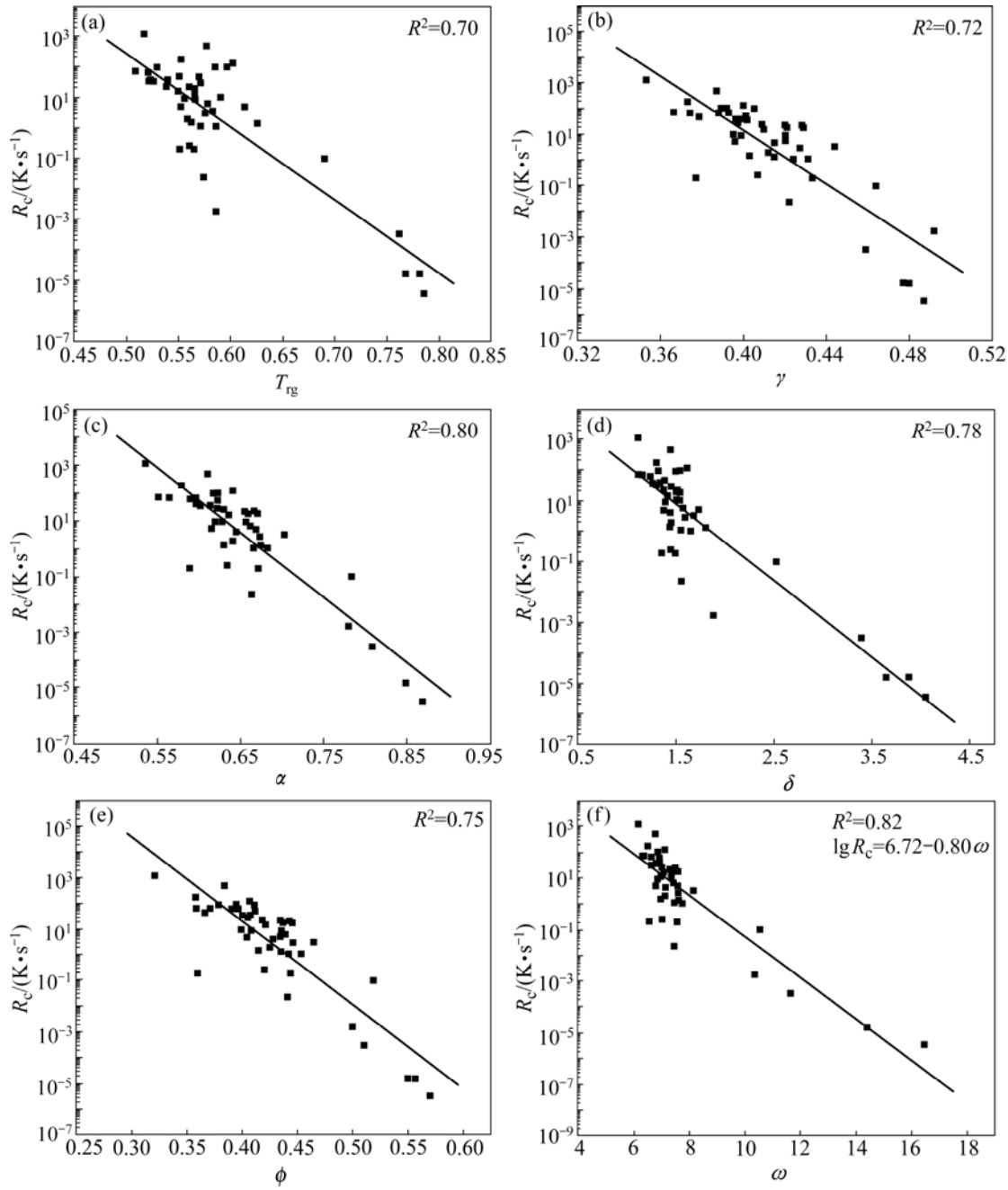

Fig.4 Correlations between R_c and T_{rg} (a), γ (b), α (c), δ (d), ϕ (e) and ω (f) for glasses including BMGs and oxides

Table 4 T_g, T_x, T_l, actual critical section thickness Z_c^{Exp} and calculated ω and Z_c^{Cal} of reported Cu-Ag-Zr-Ti alloys

Alloys	T_g/K	T_x/K	T_l/K	ω	Z_c^{Exp}/mm	Z_c^{Cal}/mm
$Cu_{60}Zr_{33}Ti_7$	740	768	1 191	7.182	3	7.7
$Cu_{54}Ag_6Zr_{33}Ti_7$	709	738	1 135	7.256	6	8.6
$Cu_{46.4}Ag_{11.6}Zr_{35}Ti_7$	689	732	1 119	7.312	6	9.2
$Cu_{44.25}Ag_{14.75}Zr_{35}Ti6$	693	730	1 112	7.345	8	9.6
$Cu_{44.25}Ag_{14.75}Zr_{36}Ti_5$	700	734	1 115	7.372	10	10.0

can be estimated approximately using Eqs.(7) and (8), respectively. Of course, these two expressions would be refined by more data of glasses to predict GFA of BMGs.

Moreover, GFA of Cu-Zr-Ti-Al alloys [22] is described by ω parameter. The characteristic temperatures of the alloys are listed together with GFA parameters in Table 5. The results of scanning electron microscopy(SEM) and X-ray diffractometry(XRD)

Table 5 Characteristic temperatures and GFA parameters of prepared Cu-Zr-Ti-Al alloys

Alloys	T_g/K	T_x/K	ΔT_x/K	T_m/K	T_l/K	T_{rg}	γ	ω
$Cu_{60}Zr_{33}Ti_7$[21]	740	768	28	1 144	1191	0.621	0.398	7.182
$(Cu_{60}Zr_{33}Ti_7)_{99}Al_1$	725	770	45	1 121	1176	0.616	0.405	7.320
$(Cu_{60}Zr_{33}Ti_7)_{97}Al_3$	714	762	48	1 117	1150	0.621	0.409	7.437
$(Cu_{60}Zr_{33}Ti_7)_{95}Al_5$	738	777	39	1 118	1186	0.622	0.404	7.326

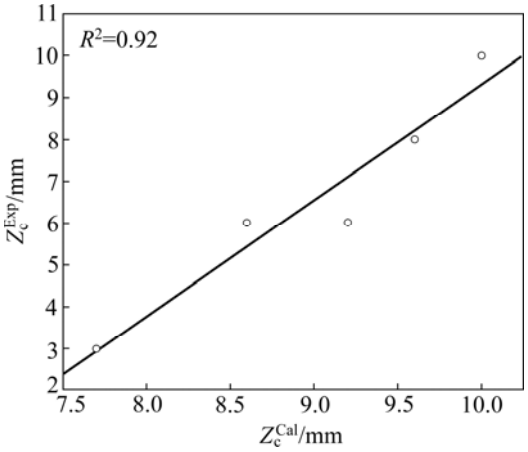

Fig.5 Actual critical section thickness Z_c^{Exp} vs calculated critical section thickness Z_c^{Cal} for Cu-based BMGs

indicated the GFA of Cu-Zr-Ti-Al alloys are enhanced firstly and then depressed with minor additions of Al. Compared with the GFA parameters in Table 5, ΔT_x, γ and ω are accordant to these experimental results, but except T_{rg}, showing that ω is one of the best applicable and reliable GFA parameters.

4 Conclusions

1) Based on the analysis of Gibbs free energy between liquid and crystal, a new GFA parameter, $\omega=T_l(T_l+T_x)/[T_x(T_l-T_x)]$, is suggested for bulk metallic glasses.

2) Together with other GFA parameters proposed formerly, including T_{rg}, γ, α, δ and ϕ, ω was verified with alloying and oxide glasses. Results indicate the new GFA parameter ω is the most reliable and applicable approach to assess the GFA of various glasses.

3) ω is applied to estimating the GFA of Cu-Ag-Zr-Ti and Cu-Zr-Ti-Al BMGs and the predicted data are consistent with the experimental results.

Acknowledgments

The authors would like to thank Dr. CAI An-hui (Institute of Powder Metallurgy, Central South University, China) for helpful discussions.

References

[1] LU Z P, BEI H, LIU C T. Recent progress in quantifying glass-forming ability of bulk metallic glasses [J]. Intermetallics, 2007, 15: 618−624.

[2] TURNBULL D. Under what conditions can a glass be formed [J]. Contemp Phys, 1969, 10(5): 473−488.

[3] INOUE A, ZHANG T, MASUMOTO T. Reductilization of embrittled La-Al-Ni amorphous alloys by viscous flow deformation in a supercooled liquid region [J]. J Non-Cryst Solids, 1993, 156/158: 598−602.

[4] LU Z P, LIU C T. A new glass-forming ability criterion for bulk metallic glasses [J]. Acta Mater, 2002, 50: 3501−3512.

[5] LU Z P, LIU C T. Glass formation criterion for various glass-forming systems [J]. Phys Rev Lett, 2003, 91: 115505 1−4.

[6] LU Z P, LIU C T. A new approach to understanding and measuring glass formation in bulk amorphous materials [J]. Intermetallics, 2004, 12: 1035−1043.

[7] MONDAL K, MURTY B S. On the parameters to assess the glass forming ability of liquids [J]. J Non-Cryst Solids, 2005, 351: 1366−1371.

[8] CHEN Q J, SHEN J, ZHANG D L, FAN H B, SUN J F, MCCARTNEY D G. A new criterion for evaluating the glass-forming ability of bulk metallic glasses [J]. Mater Sci Eng A, 2006, 433: 155−160.

[9] FAN G J, CHOO H, LIAW P K. A new criterion for the glass-forming ability of liquids [J]. J Non-Cryst Solids, 2007, 353: 102−107.

[10] KIM J H, PARK J S, LIM H K, KIM W T, KIM D H. Heating and cooling rate dependence of the parameters representing the glass forming ability in bulk metallic glasses [J]. J Non-Cryst Solids, 2005, 351: 1433−1440.

[11] TAKEUCHI A, INOUE A. Calculations of dominant factors of glass-forming ability for metallic glasses from viscosity [J]. Mater Sci Eng A, 2004, 375/377: 449−454.

[12] THOMPSON C V, SPAEPEN F. On the approximation of the free energy change of crystallization [J]. Acta Metall, 1979, 27(12): 1855−1859.

[13] LAD K N, RAVAL K G, PRATAP A. Estimation of Gibbs free energy difference in bulk metallic glass forming alloys [J]. J Non-Cryst Solids, 2004, 334/335: 259−262.

[14] MONDAL K, CHATTERJEE U K, MURTY B S. Gibbs free energy of crystallization of glass forming liquids [J]. Appl Phys Lett, 2003, 83: 671−673.

[15] CHEN H S. Metallic glasses [J]. Chinese J Phys, 1990, 28(5): 407−425.

[16] SENKOV O N, SCOTT J M, MIRACLE D B. Composition range and glass forming ability of ternary Ca-Mg-Cu bulk metallic glasses [J]. J Alloy Compd, 2006, 424: 394−399.

[17] XIAO X S, FANG S S, WANG G M, HUA Q, DONG Y D. Influence of beryllium on thermal stability and glass-forming ability of Zr-Al-Ni-Cu bulk amorphous alloys [J]. J Alloy Compd, 2004, 376: 145−148.

[18] SENKOV O N, SCOTT J M. Glass forming ability and thermal stability of ternary Ca-Mg-Zn bulk metallic glasses [J]. J Non-Cryst Solids, 2005, 351: 3087−3094.

[19] CABRAL JR A A, FREDERICCI C, ZANOTTO E D. A test of the Hruby parameter to estimate glass-forming ability [J]. J Non-Cryst Solids, 1997, 219: 182−186.

[20] LU Z P, TAN H, LI Y, NG S C. The correlation between reduced glass transition temperature and glass forming ability of bulk metallic glasses [J]. Scripta Mater, 2000, 42(7): 667−673.

[21] DAI C L, GUO H, SHEN Y, LI Y, MA E, XU J. A new centimeter-diameter Cu-based bulk metallic glass [J]. Scripta Mater, 2006, 54: 1403−1408.

[22] JI X L, PAN Y, CAI A H. The effect of Al on glass forming ability of Cu-based bulk metallic glasses [J]. J Cent South Univ Technol, 2007, 14(S2): 20−23.

(Edited by YANG Hua)